URSI GASS 2020, Rome, Italy, 29 August - 5 September 2020

Electromagnetic Scattering from a Canonical Target over an Anisotropic Rough Surface using Geometrical Optics

G. Di Martino[(1)], A. Di Simone*[(1)], W. Fuscaldo[(2)], A. Iodice[(1)], D. Riccio[(1)], and G. Ruello[(1)]
(1) Department of Information Technology and Electrical Engineering, University of Napoli "Federico II", 80125 Napoli, Italy
(2) Department of Information Engineering, Electronics and Telecommunications, Sapienza University of Rome, 00184 Rome, Italy

Abstract

In this work we provide a closed-form expression of the electromagnetic (EM) scattering from a canonical parallelepipedal target lying over an anisotropic rough surface under the Kirchhoff Approximation - Geometrical Optics solution. Starting from a recent work where we solved a similar scattering problem under the hypothesis of surface isotropy, we here generalize that model to include anistropic properties of the rough surface. The resulting formulation can be fruitfully exploited for fast evaluation of the EM field scattered from isolated buildings in built-up areas and large ships in open sea.

1 Introduction

In specific microwave remote sensing applications inherent to the urban and maritime domains, it might be helpful having a (even) rough idea of the scattering properties of large isolated targets whose geometry can be reasonably approximated as a parallelepiped. For instance, this is the case for ship target detection/classification and building parameters (height, material composition) retrieval from remote sensing data. In these contexts, numerical techniques for solving the scattering problem, such as the Method of Moments, the Finite Element Method, or the Finite-Difference Time-Domain method, are not suitable due to the high operating frequency and electrically large scene extent which would require extensive computational and/or time resources [1]. Conversely, asymptotic (high-frequency) approaches, such as Geometrical Optics (GO), can provide a fast evaluation of the overall scattered field at a cost of restricted validity limits and reduced accuracy. In [2] it was derived an analytical formulation of the backscattering problem from a canonical composite target comprising a parallelepiped lying over an isotropic background rough surface. There, the overall electromagnetic (EM) scattering from the composite target is expressed as the superposition of single- and multiple-bounce contributions which arise from the EM interaction between the target and the underlying rough surface. Analytical expressions of the single- and multiple-bounce scattering terms are derived under the general framework of the Kirchhoff Approximation (KA) and are provided for both GO and Physical Optics (PO) solutions [2]. In [3] the same scattering problem was solved under GO in a generic bistatic configuration, i.e., by assuming the transmitting and the receiving antennas no longer co-located. The larger dimensionality of the problem due to the additional dependence of the scattered field upon the scattering wavevector brings to more complicated formulas when moving from the backscattering to the bistatic geometry. However, apart from the more complicated formulation, a substantial difference between the two formulations is related to the double-scattering terms which no longer coincide in a generic bistatic configuration [3]. Both works have been exploited in building height retrieval and ship detection applications using remote sensing data [4, 5, 6, 7, 8]. However, in both previous works [2] and [3], the rough background surface is assumed isotropic, i.e., its spectrum does not exhibit directional preferences. In this work we keep the parallelepiped target model as in [2] and [3] but relax the hypothesis on the rough surface which is here assumed anisotropic. The corresponding scattering problem is derived under GO. Non-negligible anisotropy can be measured over both sea and land due to wind speed and human activities effects, respectively. The remainder of this work is as follows. Section 2 describes the geometrical and electromagnetic models of the composite target. In Section 3 some numerical results are shown and discussed, whereas concluding remarks are highlighted in Section 4.

2 Analytical Formulation of the Scattering Problem

2.1 Geometrical Model

In this work we solve the scattering problem for the canonical composite target shown in Fig. 1 along with the reference system.

The composite target includes a parallelepiped with smooth dielectric faces lying over a rough interface separating two homogeneous media. The vertical faces of the parallelepiped form an aspect or orientation angle ϕ_k with the positive x semi-axis, measured clockwise. The reference system is defined according to [3]: the xy-plane coincides with the mean plane of the rough surface, whereas the y-axis is defined such that the transmitter lies in the

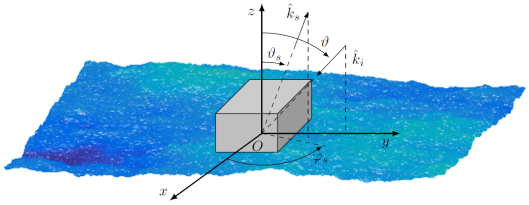

Figure 1. Geometry and reference system for the composite target.

$(y>0, z>0)$ quadrant. The rough surface is modeled as a zero-mean normally-distributed 2-dimensional stochastic process with variance σ^2 and directional power spectral density (PSD) $S(\underline{\kappa})$. Accordingly, the surface local slopes along x- and y-directions, z_x and z_y, follow a bivariate normal distribution with zero mean and covariance matrix

$$\underline{\underline{C}} = \begin{bmatrix} \sigma_x^2 & \rho\sigma_x\sigma_y \\ \rho\sigma_x\sigma_y & \sigma_y^2 \end{bmatrix}, \tag{1}$$

where σ_x and σ_y stand for the standard deviation of x- and y-slopes, respectively, and $\rho \in [0,1]$ is their correlation coefficient defined as

$$\rho = \frac{\langle z_x z_y \rangle}{\sigma_x \sigma_y}, \tag{2}$$

where $\langle \cdot \rangle$ stands for the statistical expectation. The parameters σ^2, σ_x^2, σ_y^2 and ρ can all be retrieved from the rough surface PSD $S(\underline{\kappa})$ as follows [9]

$$\sigma^2 = \int_0^{2\pi} \int_0^{\kappa_{cut}} \kappa S(\kappa,\psi)\, d\kappa\, d\psi, \tag{3}$$

$$\langle z_u z_v \rangle = \int_0^{2\pi} \int_0^{\kappa_{cut}} \kappa\kappa_u\kappa_v S(\kappa,\psi)\, d\kappa\, d\psi, \tag{4}$$

where κ and ψ are the amplitude and phase of the surface wavenumber vector $\underline{\kappa}$, κ_{cut} is the cutoff wavenumber, and the subscripts u and v in (4) can each stand for x or y and $\kappa_x = \kappa\cos\psi$, $\kappa_y = \kappa\sin\psi$.

For sea surface, the PSD can in turn be related to the wind speed v_w and direction φ_w, which is here measured counterclockwise from the positive x-axis [9]. Alternatively, the sea surface local slopes variance and correlation can be directly determined from the wind speed and direction using semiempirical formulas as illustrated in [10], thus avoiding numerical integration of (4).

2.2 Electromagnetic Model

In accordance with [2] and [3], here we assume that the incident field $\underline{E}_i(\underline{r})$ is a plane wave, i.e.,

$$\underline{E}_i(\underline{r}) = E_0 \hat{e}_i \exp(jk\hat{k}_i \cdot \underline{r}) \tag{5}$$

where E_0, $\hat{e}_i$ and $\hat{k}_i$ are the amplitude, polarization and incident propagation direction, respectively; $\underline{r}$ is the observation point, k is the EM wavenumber. In the chosen Cartesian reference system $\hat{k}_i = -\sin\theta\hat{y} - \cos\theta\hat{z}$. Accordingly, under KA-GO, the scattered field $\underline{E}_s(\underline{r})$ can be expressed as [2], [3]:

$$\begin{bmatrix} E_{\mathrm{Sh}} \\ E_{\mathrm{Sv}} \end{bmatrix} = jk\frac{e^{jkr}}{4\pi r} \begin{pmatrix} S_{\mathrm{hh}} & S_{\mathrm{vh}} \\ S_{\mathrm{hv}} & S_{\mathrm{vv}} \end{pmatrix} \begin{bmatrix} E_{0\mathrm{h}} \\ E_{0\mathrm{v}} \end{bmatrix} I_{A_0}, \tag{6}$$

where $E_{0\mathrm{h}}$ and $E_{0\mathrm{v}}$ stand for the amplitudes of the horizontal and vertical components of the incident electric field $\underline{E}_{\mathrm{i}}$, respectively; the scattering matrix $\underline{\underline{S}}$ accounts for the polarization states of the transmitter and receiver and depends upon the incident $\hat{k}_i$ and scattered $\hat{k}_s$ propagation directions, while it does not depend upon the statistical description of the surface [2], [3]. Finally, the scattering integral I_{A_0} can be written as follows

$$I_{A_0} = \iint_{A_0} e^{jk(\eta_x x + \eta_y y + \eta_z z(x,y))}\, dxdy \tag{7}$$

where $\underline{\eta} = \hat{k}_i - \hat{k}_s$, $\hat{k}_s = \sin\theta_s\cos\phi_s\hat{x} + \sin\theta_s\sin\phi_s\hat{y} + \cos\theta_s\hat{z}$ is the scattering direction and I_{A_0} accounts for the statistical description of the surface height $z(x,y)$. It is noteworthy that, under KA-GO, the single bounce from the upper horizontal face of the target is a deterministic function of the incident direction and target sizes: actually, it is not influenced by the underlying rough surface. Therefore, its expression is not reported here for the sake of brevity and can be found in [3]. However, the overall EM field scattered from the composite target is a stochastic process due to the interactions between the target and the rough surface. Closed-form expressions can be derived for the mean value and the mean squared value of the scattered field, which are of interest here. According to (6), the scattered EM field relevant to the single- and multiple-bounce terms is completely characterized by the scattering matrix and the scattering integral. However, here we focus on the evaluation of the scattering integral only, as it is the only factor in (6) which is influenced by the directional properties of the surface spectrum. Indeed, the expressions of the scattering matrix presented in [3, Tables I-V] still hold here and are not reported for the sake of brevity. Moreover, the rationale for the evaluation of the scattering integral relevant to the different bounces provided in [3] still holds as well. However, the final expressions are slightly different as the rough surface is no longer isotropic. Under KA-GO, the mean value of the scattering integral $\langle I_{A_0} \rangle$ is related to the characteristic function of the rough surface height $z(x,y)$ which keeps the same formal expression when moving to anisotropic surfaces. Accordingly, the coherent component of the overall scattered field can still be expressed as in [3]. Conversely, the incoherent component of each scattering term is proportional to the probability density function of local surface slopes, see the exponential terms in $\langle |I_{A_0}|^2 \rangle$ in [3, Tables I-V]. By introducing the anisotropy of the rough surface, the mean squared value of the scattering integral for any bounce can be expressed in a compact form as follows

$$\langle |I_{A_0}|^2 \rangle = A_0 \frac{2\pi}{\eta_z^2 k^2 \sigma_x\sigma_y\sqrt{1-\rho^2}} \times \exp\left[-\frac{\sigma_y^2\eta_x^2 + \sigma_x^2\eta_y^2 - 2\rho\sigma_x\sigma_y\eta_x\eta_y}{2\eta_z^2\sigma_x^2\sigma_y^2(1-\rho^2)} \right] \tag{8}$$

where A_0 is the area of the portion of rough surface contributing to the scattered field. Correlation properties of the local slopes do not affect the rough surface area participating to the overall field scattered from the composite target. Therefore, its expression coincide with that derived for isotropic surface and are reported in [3, Tables I-V] for all the bounces. For instance, $A_0 = ab$ for the single bounce from the rough surface, where a and b are the sizes of the illuminated portion of the rough surface. For multiple bounces, the shadowing effects of the target must be accounted for. Consequently, for higher-order bounces, A_0 depends on the incident and scattering directions, target size and orientation [3]. The vector difference $\underline{\eta}$ varies among the different bounces due to the reflections on the target vertical face. Its definitions are provided in [3, Appendix]. For the sake of clarity, here we report its expressions in terms of angles. For the single scattering contribution from the rough surface $\underline{\eta} = \hat{k}_i - \hat{k}_s$, i.e.

$$\eta_x = -\sin\theta_s\cos\phi_s \tag{9a}$$
$$\eta_y = -\sin\theta - \sin\theta_s\sin\phi_s \tag{9b}$$
$$\eta_z = -\cos\theta - \cos\theta_s \tag{9c}$$

For the double-bounce contribution wall-ground (WG)

$$\eta_x = \sin\theta\sin\phi_k - \sin\theta_s\cos(\phi_s+\phi_k) \tag{10a}$$
$$\eta_y = \sin\theta\cos\phi_k - \sin\theta_s\sin(\phi_s+\phi_k) \tag{10b}$$
$$\eta_z = -\cos\theta - \cos\theta_s \tag{10c}$$

whereas for the double-bounce contribution ground-wall (GW)

$$\eta_x = -\sin\theta_s\cos(\phi_s+2\phi_k) \tag{11a}$$
$$\eta_y = -\sin\theta + \sin\theta_s\sin(\phi_s+2\phi_k) \tag{11b}$$
$$\eta_z = -\cos\theta - \cos\theta_s \tag{11c}$$

It is worth noting that, as opposed to the isotropic case, anisotropic surfaces make the term $\langle|I_{A_0}|^2\rangle$ relevant to WG no longer coincide with that in GW. Indeed, for the isotropic surface the exponential term in (8) depends on the term $(\eta_x^2+\eta_y^2)/\eta_z^2$ which is the same in WG and GW. Finally, for the triple bounce scattering term

$$\eta_x = \sin\theta\sin\phi_k - \sin\theta_s\cos(\phi_s+\phi_k) \tag{12a}$$
$$\eta_y = \sin\theta\cos\phi_k + \sin\theta_s\sin(\phi_s+\phi_k) \tag{12b}$$
$$\eta_z = -\cos\theta - \cos\theta_s \tag{12c}$$

The radar cross section (RCS) of the composite target is then evaluated as

$$\mathrm{RCS} = 4\pi r^2\frac{\langle|\underline{E}_s(\underline{r})|^2\rangle}{|E_0|^2} \tag{13}$$

where the different scattering contributions are summed up as illustrated in [2, Section VII]. Finally, it is worth mentioning that the anistropic properties of the rough surface do not modify the validity limits reported in [3, Appendix] for isotropic surface.

Table 1. Simulation parameters

Parameter	Value
Frequency	1.5GHz
Wind speed	10 m/s
Wind direction	varying
Incidence angle	30°
Sea spectrum	Elfouhaily
Ship orientation	0°
Ship size	$100\times30\times20$ m^3
Seawater relative permittivity	$70.26 - j39.94$
Ship relative permittivity	$4.45 - j2.72\times10^7$

3 Numerical Results

In this Section we show some numerical results in order to visualize the impact of the surface anisotropy on the RCS of the composite target. Simulation parameters are listed in Table 1. Here we focus on the simulation of a ship target over sea surface, whose statistics are here described by the Elfouhaily directional spectrum [9]. Figure 2 shows the RCS of the composite target in the θ_s-ϕ_s plane for horizontal-transmit horizontal-receive (HH) polarization and for φ_w ranging from 0° to 180° with angular steps of 30°. Indeed, the Elfouhaily directional spectrum depends upon the direction of the wind but not upon its sense, therefore, $\varphi_w \in [0°, 180°]$ can be considered to investigate the whole directional preferences. Accordingly, results for $\varphi_w = 0°$ and $\varphi_w = 180°$ coincide, see Fig. 2. It emerges that the wind direction modifies the angular distribution of the EM energy scattered from the target, whereas the single scattering contribution from the ship deck remains unchanged, see the bright return around $\phi_s = 270°$. However, a strong return is still localized around the backscattering direction $\theta_s = \theta$ and $\phi_s = 90°$ as in the isotropic case [3].

4 Conclusions

This work presents an analytical model for fast evaluation of the EM scattering from a canonical composite target comprising a parallelepiped with smooth dielectric faces and lying over a rough surface. With respect to the existing literature dealing with similar canonical problems, the main novelty consists in the anisotropy of the rough surface, which is here modeled as a normally-distributed process with directional spectrum. The scattered field is evaluated by means of KA-GO and then decomposed in single- and multiple-bounce scattering contributions, whose mean and mean squared values are discussed here. Numerical simulations of maritime environments show the impact of the anistropy of the background sea surface on the RCS of the ship target. Future research lines may regard the derivation of analytical models under different roughness regimes, i.e., KA-PO.

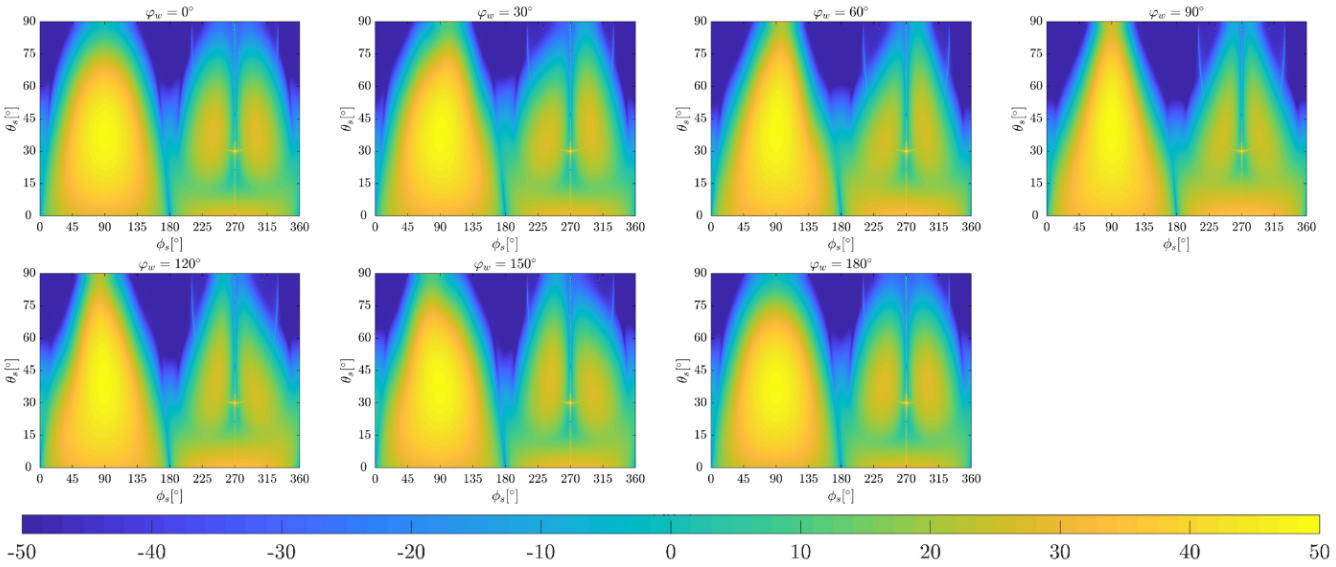

Figure 2. RCS of the composite target in the θ_s-ϕ_s plane for HH polarization and assuming wind direction φ_w from 0° to 180° with step of 30°. Remaining parameters are set according to Table 1.

5 Acknowledgements

This research has been funded by the Department of Information Technology and Electrical Engineering of the University of Napoli, "Federico II", in the framework of the MORES project.

References

[1] R. F. Harrington, *Time-Harmonic Electromagnetic Fields*. New York, NY, USA: McGraw-Hill, 1961.

[2] G. Franceschetti, A. Iodice, and D. Riccio, "A canonical problem in electromagnetic backscattering from buildings," *IEEE Transactions on Geoscience and Remote Sensing*, vol. 40, no. 8, pp. 1787–1801, 2002.

[3] A. Di Simone, W. Fuscaldo, L. M. Millefiori, D. Riccio, G. Ruello, P. Braca, and P. Willett, "Analytical models for the electromagnetic scattering from isolated targets in bistatic configuration: Geometrical Optics solution," *IEEE Transactions on Geoscience and Remote Sensing*, vol. 58, no. 2, pp. 861–880, Feb. 2020.

[4] A. Di Simone, L. M. Millefiori, G. Di Martino, A. Iodice, D. Riccio, G. Ruello, P. Braca, and P. Willett, "Spaceborne GNSS-reflectometry for ship-detection applications: Impact of acquisition geometry and polarization," in *IGARSS 2018-2018 IEEE International Geoscience and Remote Sensing Symposium*. IEEE, 2018, pp. 1071–1074.

[5] T. Beltramonte, P. Braca, M. Di Bisceglie, A. Di Simone, C. Galdi, A. Iodice, L. M. Millefiori, D. Riccio, and P. Willett, "Simulation-based feasibility analysis of ship detection using GNSS-R delay-doppler maps," *Journal of Selected Topics in Applied Earth Observations and Remote Sensing*, vol. PP, no. 99, 2020.

[6] P. Iervolino, R. Guida, and P. Whittaker, "A model for the backscattering from a canonical ship in SAR imagery," *IEEE Journal of Selected Topics in Applied Earth Observations and Remote Sensing*, vol. 9, no. 3, pp. 1163–1175, 2016.

[7] P. Iervolino and R. Guida, "A novel ship detector based on the generalized-likelihood ratio test for SAR imagery," *IEEE Journal of Selected Topics in Applied Earth Observations and Remote Sensing*, vol. 10, no. 8, pp. 3616–3630, 2017.

[8] R. Guida, A. Iodice, and D. Riccio, "Height retrieval of isolated buildings from single high-resolution sar images," *IEEE Transactions on Geoscience and Remote Sensing*, vol. 48, no. 7, pp. 2967–2979, 2010.

[9] T. Elfouhaily, B. Chapron, K. Katsaros, and D. Vandemark, "A unified directional spectrum for long and short wind-driven waves," *Journal of Geophysical Research: Oceans*, vol. 102, no. C7, pp. 15 781–15 796, 1997.

[10] G. Di Martino, A. Iodice, and D. Riccio, "Closed-form anisotropic polarimetric two-scale model for fast evaluation of sea surface backscattering," *IEEE Transactions on Geoscience and Remote Sensing*, vol. 57, no. 8, pp. 6182–6194, 2019.